

# Clustering mutants favor and disfavor fixation

Yunming Xiao, Bin Wu\*

School of Sciences, Beijing University of Posts and Telecommunications, China

\* bin.wu@bupt.edu.cn

## Abstract

Exploration of the emerging patterns of mutants in a finite wild-type group on spatial structure is an attracting topic. The mutation is assumed to appear with a low probability. Many studies have investigated the expansion and invasion chances for a few mutants under different games on spatial structures. It is shown that different games could lead to different evolving patterns. There are rules generalized for when the process favors the mutants, where many of the rules indicate that clustering plays a heavy role in the expansion of mutants. However, on the one hand, clustering hasn't been considered as an independent variable and is ignored in some previous analysis, where the patterns of the games might be affected by clustering and thus might not be well compared. On the other hand, many simulations for exploring the clustering effects are analytically intractable due to the great complexity of calculation and the difficulty to find proper categorizations on complex spatial structures. In order to explore the solely and fundamental effect of the clustering, we employ a minimal model where no game is involved and a simple cycle is adopted. In this way, we disentangle the clustering and the games. The applied process reflects very nontrivial effects of the clustering. Our results show the assortment is an amplifier of the selection for the connected mutants compared with the separated ones. Nevertheless, as mutants are separated, the more dispersed they are, the greater chance of invasion is. The non-monotonical affection of clustering is quite unintuitive. And what it affects under the minimal model reveals the great potential effects and also the great complexity of clustering when games are involved. We also notice an uncoordination between the fixation probability and fixation time for mutants.

## Author summary

Our adopted cycle model is quite simple but is capable of reflecting the solely role of clustering. The ravel of the games and clustering creates a new angle into the question and it should be the building block for further exploration. Though the connected mutants case is well explored by many studies, a little modification, as the separated mutants cases, brings the problem to a greater complexity. With the help of our developed algorithm, we are enabled to explore the fixation probability and fixation time for larger population and then generalize some regularities. Our analytical and numerical results show the fundamental and nontrivial effect of the clustering, which should be considered when studying the emerging patterns of mutants for different games on spatial structures.

# Introduction

Cooperation is frequently observed in the natural world ranging from micro community to human society. Yet it is seemingly against evolutionary theory, since cooperators forgo their own benefit to benefit others whereas defectors take no cost. For the past two decades, it has been intensively investigated how cooperation is evolved via natural selection [1, 4, 8, 11–13]. Spatial reciprocity assumes that individuals only interact with thy neighbors, and selection happens locally rather over the entire population [1].

For network reciprocity, a surprisingly simple rule is obtained [2] that cooperation is favored provided the benefit-to-cost ratio exceeds the average number of neighbors per individual. It holds for death-birth process under weak selection limit. A key intermediate step to achieve this simple rule is that under weak selection limit, a cooperator would have more cooperator neighbors than defector neighbors. Furthermore, the few neighbors a cooperator has, the more proportion of cooperator neighbors a cooperator has. In other words, few neighbors per individual lead to a clustering of the cooperators for evolutionary dynamics on a network. Intuitively a cooperator surrounded by many cooperator neighbors obtain high payoff. In fact, it has been found that evolutionary dynamics on a network would result in an assortment of individuals using the same strategies. It paves the way to solve many social dilemmas including those modelled by multiple-player games. The assortment of cooperators has been intensively employed to investigate the fixation probability and the fixation time for stochastic evolutionary game dynamics on a network. Besides, other mechanisms promoting cooperation also results in the assortment of cooperators, which is similar to the network reciprocity. Therefore, it would be necessary to investigate how the assortment alters the evolutionary outcome.

For previous studies on the evolution of cooperation on a network, both the game interaction and assortment are taken into account. Herein cooperation is modelled as a social dilemma via dyadic or multi-player game. Whereas assortment of cooperators follows as a result of weak selection limit. It is still far from clear how assortment alone changes the fate of evolution. In this paper, we try to disentangle the game dynamics and the clustering. And we employ a minimal model to explore this issue. We only consider the frequency-independent cases, without any games involved, to explore the role that the clustering plays alone. As a first step, we adopt a circle as the underlying population structure. Our study starts with two mutants. They have an initial distance denoting the number of wild-type individuals between them. We regard the distance as a measure of clustering. And we explore that how the assortment of mutants alter the fixation probability and fixation time analytically.

## The Model

### Connected Mutants

Assume there are  $N$  individuals with two strategies for each, A (wild-type) and B (mutant). The corresponding fitness are  $f_A$  and  $f_B$  respectively. All the individuals are located on a ring. In other words, every individual has exactly two neighbors. In this paper, we consider a frequency-independent process, where the individual fitness is solely determined by its strategy. An example of DB process is illustrated in Fig. 1, where  $N = 6$ . The process can be described by a one-dimensional Markov Chain. The weight  $w$  denotes the number of individuals who adopt the mutant strategy. Each weight corresponds to a state  $S_w$  in the Markov Chain. The Markov Chain contains two absorbing states ( $w_0$  and  $w_6$ ) and the other states ( $w_i$ , where  $1 \leq i \leq 5$ ) belong to one equivalence class.

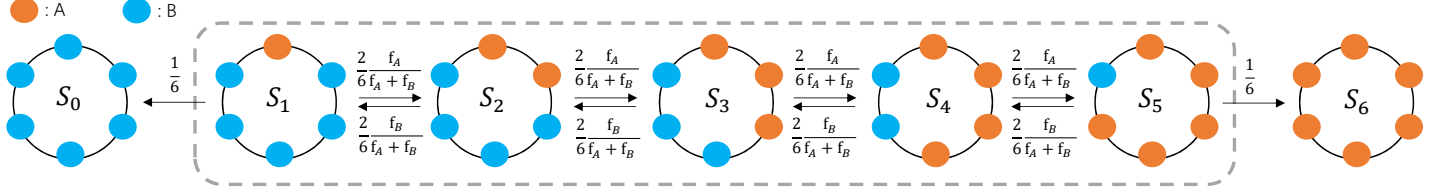


**Fig 1.** The death-birth process where population size  $N = 6$ , starting from one initial mutant individual. The states in the dashed box belong to the same one equivalence class whereas two states outside the box are absorbing states.

Using  $P_{a,b}$  to denote the probability of changing from state  $S_a$  to  $S_b$ , the well-known Kolmogorov backward equation is written as

$$\pi_w = P_{w,w+1}\pi_{w+1} + P_{w,w-1}\pi_{w-1} + (1 - P_{w,w+1} - P_{w,w-1})\pi_w, \quad (1)$$

with  $\pi_0 = 0$  and  $\pi_N = 1$ .

This is the well-known Kolmogorov backward equations, and  $\pi_w$  is the fixation probability for  $S_w$ . Solving the Kolmogorov backward equation, the fixation probability can be obtained:

$$\pi_w = \frac{1 + \sum_{j=1}^{w-1} \prod_{k=1}^j \gamma_k}{1 + \sum_{w=1}^{N-1} \prod_{k=1}^j \gamma_k}, \quad (2)$$

where

$$\gamma_w = \frac{P_{w,w-1}}{P_{w,w+1}}. \quad (3)$$

Let  $r$  denote the fraction of fitness of two strategies, i.e.,  $\frac{f_A}{f_B} = r$ . It holds as follows:

$$\gamma_w = \begin{cases} \frac{r+1}{2r}, & w = 1 \\ \frac{1}{r}, & w = 2, \dots, N-2 \\ \frac{2}{r+1}, & w = N-1 \end{cases} \quad (4)$$

Applying Eq. (2) with Eq. (4) and the condition  $N = 6$ , the fixation probabilities are then obtained. In later sections, we would discuss the effect of clustering and other processes with two initial mutant individuals are considered. Here, we list the fixation probability for initial two connected mutants as follows:

$$\pi_2 = \frac{r^3(1+3r)}{3+2r+2r^2+2r^3+3r^4}. \quad (5)$$

Let  $\tau_i^A$  denote the conditional fixation time from state  $S_i$  to  $S_N$ . We have

$$\pi_i \tau_i^A = P_{i,i-1}\pi_{i-1}(\tau_{i-1}^A + 1) + (1 - P_{i,i-1} - P_{i,i+1})\pi_i(\tau_i^A + 1) + P_{i,i+1}\pi_{i+1}(\tau_{i+1}^A + 1),$$

with  $\pi_0 \tau_0^A = 0$  and  $\tau_N^A = 0$ . (6)

Solving the recursive equations, we obtain

$$\tau_i^A = \tau_1^A \frac{\pi_1}{\pi_i} \sum_{k=1}^{i-1} \prod_{m=1}^k \gamma_m - \sum_{k=1}^{i-1} \sum_{l=1}^k \frac{1}{\pi_i} \frac{\pi_l}{P_{l,l+1}} \prod_{m=l+1}^k \gamma_m,$$

(7)

with  $\tau_1^A = \sum_{k=1}^{N-1} \sum_{l=1}^k \frac{\pi_l}{P_{l,l+1}} \prod_{m=l+1}^k \gamma_m$ .

Taking  $N = 6$  into the above equation, we obtain

$$\tau_2^A = \frac{3(11 + 75r + 132r^2 + 140r^3 + 109r^4 + 45r^5)}{(1 + 3r)(3 + 2r + 2r^2 + 2r^3 + 3r^4)}. \quad (8)$$

### Separated Mutants For Small Circle

To explore the effect of clustering, we consider the process that there are two mutants with a distance  $d$ . That is to say, there are  $d$  connected wild-type individuals locating between two mutant individuals. In this section, we take the case where  $N = 6$  for a detailed exploration. Note that a population of 6 individuals is the minimal requirement here since a smaller graph contains only one or zero possible not fully connected states, as shown in Fig. 2.

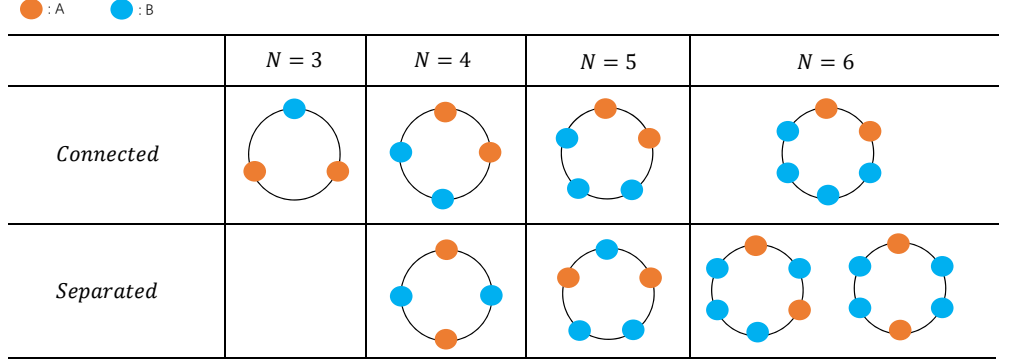


**Fig 2. The possible states for two mutant individuals in different population sizes. Starting from a population of size 6, two and more states are involved.**

As illustrated in Fig. 3, the process gives rise to more states than that which simply starts with two connected mutant individuals. Comparing with the previous process in Fig. 1, we divide all the states into two sets: the middle-state set  $S$  and the final-state set  $F$ . The middle states refer to all the states with two separated groups of mutant individuals whereas the final states contain only one mutant group. Note that a group refers to some connected individuals with the same strategy. Fig. 3 shows four properties of the process: i) all the middle states can reach each other and they belong to one equivalence class. ii) The final states can also reach each other and the final-state-set contains another equivalence class ( $F_i, 1 \leq i \leq 5$ ) and two absorbing states ( $F_0$  and  $F_6$ ). iii) The middle states can reach final states in limited time, however, the final states cannot reach any of the middle states. iv) We find that the middle states are transient (sooner or later, they will evolve into one of the final states). The Markov Chain, as a mathematical means to express the process in the figure, is not one-dimensional anymore. These features lead to a mathematical challenge.

● : A   ● : B

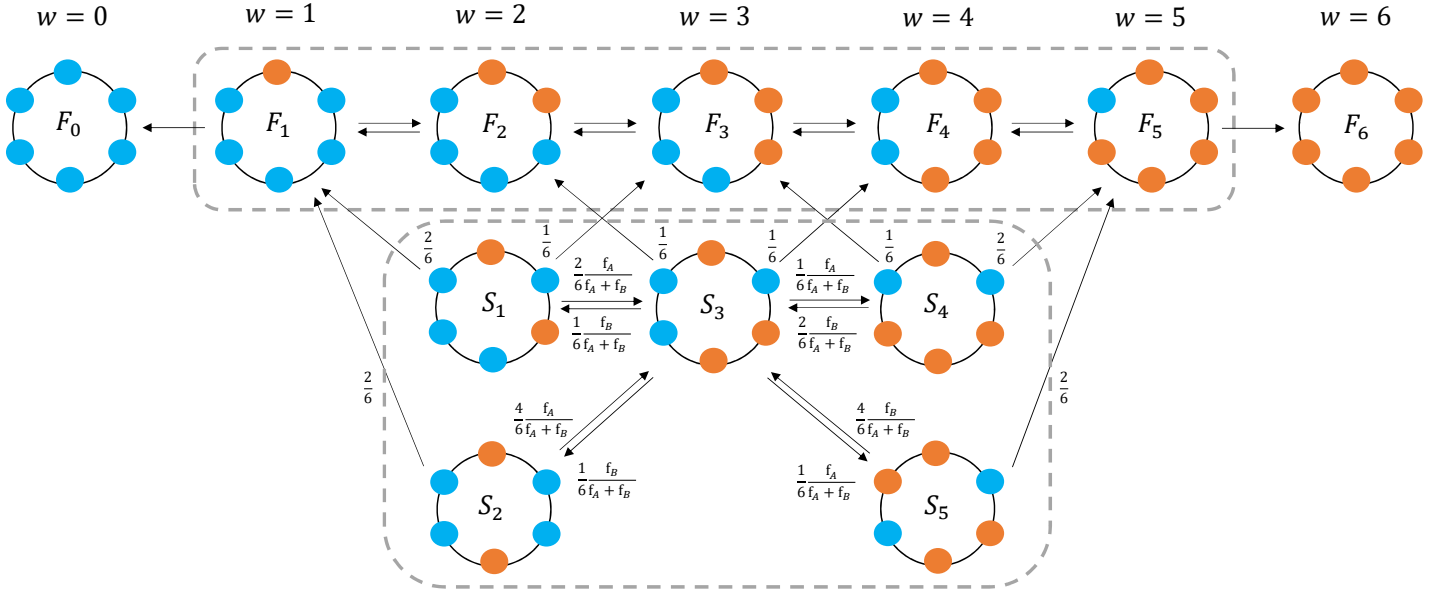


**Fig 3.** The states and transition probabilities of the death-birth process with two separated mutant individuals in a population of 6. The  $w$  refers to the weight of the mutant individuals.

The transition matrix  $P$  for the process in Fig. 3 is listed as follows:

$$\begin{array}{c|ccccc|ccccc|ccccc}
 & S_1 & S_2 & S_3 & S_4 & S_5 & F_0 & F_1 & F_2 & F_3 & F_4 & F_5 & F_6 \\
 \hline
 S_1 & \frac{1}{6} \frac{3+r}{1+r} & 0 & \frac{1}{6} \frac{2r}{1+r} & 0 & 0 & 0 & \frac{1}{3} & 0 & \frac{1}{6} & 0 & 0 & 0 \\
 S_2 & 0 & \frac{1}{6} \frac{4}{1+r} & \frac{1}{6} \frac{1}{4r} & 0 & 0 & 0 & 0 & \frac{1}{3} & 0 & 0 & 0 & 0 \\
 S_3 & \frac{1}{6} \frac{1}{1+r} & \frac{1}{6} \frac{1}{1+r} & \frac{1}{6} \frac{1+2r}{1+r} & \frac{1}{6} \frac{r}{1+r} & \frac{1}{6} \frac{r}{1+r} & 0 & 0 & \frac{1}{6} & 0 & \frac{1}{6} & 0 & 0 \\
 S_4 & 0 & 0 & \frac{1}{6} \frac{1+r}{1+r} & \frac{1}{6} \frac{2+r}{1+r} & 0 & 0 & 0 & 0 & 0 & \frac{1}{6} & 0 & \frac{1}{3} \\
 S_5 & 0 & 0 & \frac{1}{6} \frac{4}{1+r} & 0 & \frac{1}{6} \frac{4r}{1+r} & 0 & 0 & 0 & 0 & 0 & 0 & 0 \\
 \hline
 F_0 & 0 & 0 & 0 & 0 & 0 & 1 & 0 & 0 & 0 & 0 & 0 & 0 \\
 F_1 & 0 & 0 & 0 & 0 & 0 & \frac{1}{6} & \frac{5+3r}{1+r} & \frac{1}{6} \frac{2r}{1+r} & 0 & 0 & 0 & 0 \\
 F_2 & 0 & 0 & 0 & 0 & 0 & 0 & \frac{1}{6} \frac{2}{1+r} & \frac{4}{6} & 0 & \frac{1}{6} \frac{2r}{1+r} & 0 & 0 \\
 F_3 & 0 & 0 & 0 & 0 & 0 & 0 & 0 & \frac{1}{6} \frac{2}{1+r} & \frac{2}{6} & \frac{1}{6} \frac{1+r}{1+r} & 0 & 0 \\
 F_4 & 0 & 0 & 0 & 0 & 0 & 0 & 0 & 0 & \frac{1}{6} \frac{1+r}{1+r} & \frac{4}{6} & \frac{2}{6} \frac{1+r}{1+r} & 0 \\
 F_5 & 0 & 0 & 0 & 0 & 0 & 0 & 0 & 0 & 0 & \frac{1}{6} \frac{2r}{1+r} & \frac{1}{6} \frac{3+5r}{1+r} & \frac{1}{6} \\
 F_6 & 0 & 0 & 0 & 0 & 0 & 0 & 0 & 0 & 0 & 0 & 0 & 1
 \end{array} \tag{9}$$

Denote the fixation probability starting from state  $i \in \{S, F\}$  whereas ending up with state  $F_6$  as  $\Psi_i$ . Based on the property of the Markov Chain, the following holds:

$$\Psi_i = \sum_{j \in \{S, F\}} P_{i,j} \Psi_j, \quad \forall i \in \{S, F\}. \tag{10}$$

It is equivalence to

$$\Psi = P\Psi, \tag{11}$$

with boundary conditions  $\Psi_{F_0} = 0$  and  $\Psi_{F_6} = 1$  (subject to the property ii).

We divide the states into two sets: the middle-state set  $S$  and the final-state set  $F$ . Thus, we have  $\Psi = (\Psi_S \ \Psi_F)$ . And the one-step transition matrix  $P$  can be written as four

parts, as the two crossing lines in Eq. (9) illustrates,

$$P = \begin{matrix} S & F \\ S & F \end{matrix} \begin{pmatrix} Q_1 & Q_2 \\ 0 & Q_3 \end{pmatrix}. \quad (12)$$

This corresponds to the process property iii). Considering a transition from the middle states to the final states, we find that such transition requires a "collapse" of two separate groups with the same strategy. Take the transition from  $S_1$  to  $F_1$  as an example, the transition occurs when a mutant is chosen to die with probability  $\frac{2}{6}$ . The chosen mutant has two wild-type neighbors. The chosen mutant will be replaced by a wild-type offspring. It is a collapse of the two wild-type groups. This shows that the transition probability from  $S_1$  to  $F_1$  is independent on the relative fitness of the mutant  $r$ . In general, this applies to any transition from the middle-state set  $S$  to final-state set  $F$ . That is to say,  $Q_2$  is independent of mutant fitness  $r$ . Similarly,  $Q_1$  and  $\Psi$  are dependent on  $r$ .

Taking Eq. (12) into Eq. (11), we obtain

$$\begin{cases} \Psi_S = Q_1 \Psi_S + Q_2 \Psi_F \\ \Psi_F = Q_3 \Psi_F \end{cases}. \quad (13)$$

Note that the second equation ( $\Psi_F = Q_4 \Psi_F$ ) is the same as Eq. (1). Thus we have  $\Psi_F = \pi$ .

We now consider the first equation ( $\Psi_S = Q_1 \Psi_S + Q_2 \Psi_F$ ), which can be transferred to  $(I - Q_1) \Psi_S = Q_2 \Psi_F$ . We show that  $I - Q_1$  is reversible in the following. Since all the middle states are transient with respect to process property i) and iv), we have  $\sum_{t=0}^{\infty} P_{ij}^{(t)} < \infty, \forall i, j \in S$  [3]. This is equivalent to

$$\left( \sum_{t=0}^{\infty} Q_1^t \right)_{ij} < \infty. \quad (14)$$

Let  $H = \sum_{t=0}^{\infty} Q_1^t$ , and we know  $H$  exists. Notice that

$$H(I - Q_1) = \sum_{t=0}^{\infty} Q_1^t (I - Q_1) = \sum_{t=0}^{\infty} Q_1^t - \sum_{t=1}^{\infty} Q_1^t = I, \quad (15)$$

where  $I$  is the identity matrix with the same size as that of  $Q_1$ . We then acknowledge that  $H = (I - Q_1)^{-1}$ . Thus, it holds

$$\Psi_S = (I - Q_1)^{-1} Q_2 \Psi_F. \quad (16)$$

In the process of Fig. 3, the fixation probabilities of states with two separated mutants are listed as follows:

$$\begin{cases} \Psi_{S_1} = \frac{r^2(28 + 167r + 475r^2 + 920r^3 + 1036r^4 + 585r^5 + 117r^6)}{(3 + 2r + 2r^2 + 2r^3 + 3r^4)(45 + 210r + 322r^2 + 210r^3 + 45r^4)} \\ \Psi_{S_2} = \frac{r^2(39 + 179r + 456r^2 + 896r^3 + 1041r^4 + 597r^5 + 120r^6)}{(3 + 2r + 2r^2 + 2r^3 + 3r^4)(45 + 210r + 322r^2 + 210r^3 + 45r^4)} \end{cases}. \quad (17)$$

Expanding the equations around the neural selection, i.e.  $r = 1$ , gives rise to

$$\begin{cases} \Psi_{F_2} (= \pi_2) = \frac{2}{6} + \frac{7}{12}(r-1) - \frac{40}{288}(r-1)^2 + o((r-1)^3) \\ \Psi_{S_1} = \frac{2}{6} + \frac{6}{12}(r-1) - \frac{49}{288}(r-1)^2 + o((r-1)^3), \\ \Psi_{S_2} = \frac{2}{6} + \frac{6}{12}(r-1) - \frac{46}{288}(r-1)^2 + o((r-1)^3) \end{cases}, \quad (18)$$

where  $\pi_2$  is obtained in Eq. (5). Note that  $F_2$  denotes the process with two connected individuals, or say  $d = 0$ , while  $S_1$  and  $S_2$  here refer to the processes where two mutant individuals are in a distance of 1 and 2 respectively.

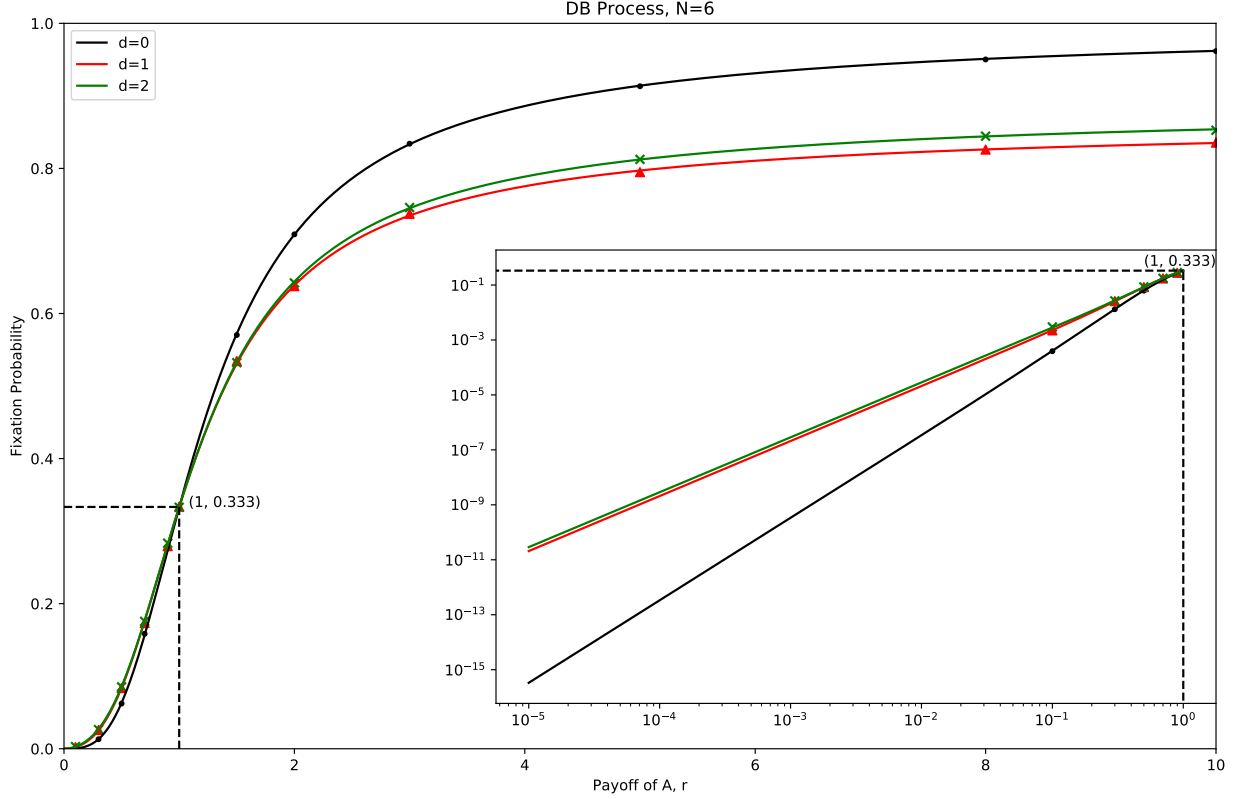


**Fig 4.** The fixation probability for  $N = 6$  with different initial mutant distances  $d$ . The curve is drawn by the analytical results whereas the points are simulation results.

In general, we find four features of Eq. (18). i) All the three results share the same constant part in the expansions and they are equal to the proportion of mutant individuals. That is to say, for a neutral selection, i.e.  $r = 1$ , the fixation probabilities are only determined by the number of the mutants. ii) The first-order derivatives of fixation probabilities for separated mutants ( $S_1$  and  $S_2$ ) are both equal to  $\frac{6}{12}$ . It shows that the fixation probability overlaps for different initial distances when the selection intensity is small (see Fig. 4). iii) The first-order derivatives of fixation probabilities for separated mutants ( $\frac{d}{dr}\Psi_{S_1} = \frac{d}{dr}\Psi_{S_2} = \frac{6}{12}$ ) are greater than 0, but are smaller than that of the connected mutants ( $\frac{d}{dr}\Psi_{F_2} = \frac{7}{12}$ ). This indicates a slower change for the separated mutants than the connected mutants when the fitness of mutant becomes other than 1, as Fig. 4 shows. In particular, when  $r < 1$ , which refers to that the mutant individuals are at disadvantage for survival, the fully connected mutants weaken the overall fixation probability. On the contrary, the fully connected mutants greatly promote the invasion when they are at advantage (i.e.,  $r > 1$ ). iv) Moreover, considering the processes that the initial mutants are separated. The second-order derivative of the fixation probability for  $d = 1$  ( $\frac{d^2}{dr^2}\Psi_{S_1} = -\frac{49}{288}$ ) is smaller than that for  $d = 2$  ( $\frac{d^2}{dr^2}\Psi_{S_2} = -\frac{46}{288}$ ). Thus, when  $r$  is much greater than or much smaller than one, the

closer the two mutants are, the weaker the invasion is. Note that the results tell that the rank of the invasion chance is determined solely by the clustering factor (i.e., the distance of two mutants) as long as mutants are not fully connected.

We now investigate the time to fixation for mutants. Let  $\tau_i^A$  denote the conditional fixation time from state  $i \in \{S, F\}$  to  $F_6$ .  $T^A$  is an array of  $\tau_i^A$  and we list the states  $i$  in an order that is the same as in  $\Psi$ . That is to say,  $T^A = (\frac{T_S^A}{T_F^A})$ , where  $T_S^A$  is the conditional fixation time to  $F_6$  for the middle states and  $T_F^A$  is that for the final states. For state  $i \in \{S, F\}$ , we have

$$\begin{aligned} \Psi_i \cdot \tau_i^A &= \sum_{j \in \{S, F\}} \Psi_j \cdot P_{i,j} \cdot (\tau_j^A + 1), \\ \text{with } \tau_{F_6}^A &= 0 \text{ and } \Psi_{F_0} \cdot \tau_{F_0}^A = 0. \end{aligned} \quad (19)$$

The right side of the equation contains all the cases that one-step further from  $S_1$ , weighted by the one-step transition probabilities.

Symbol  $\circ$  is the expression of Hadamard product. In particular, for two matrix  $A = [a_{ij}]$  and  $B = [b_{ij}]$  with the same shape, we have  $A \circ B = [a_{ij} \cdot b_{ij}]$ . We then transfer the Eq. 19 to

$$\Psi \circ T^A = P[\Psi \circ (T^A + \mathbf{1})], \quad (20)$$

where  $\mathbf{1}$  is an array of value 1 with the same dimensions as  $T^A$ . This is equivalent to

$$\Psi \circ T^A = P \cdot (\Psi \circ T^A) + P \cdot \mathbf{1}. \quad (21)$$

And moving all elements with  $\Psi \circ T$  to the left side, we have

$$(I - P) \cdot (\Psi \circ T^A) = P \cdot \mathbf{1}, \quad (22)$$

where  $I$  denotes the identity matrix.

Splitting the middle states and final states always benefits a lot in our study case, then Eq. 22 is

$$\begin{pmatrix} I - Q_1 & -Q_2 \\ 0 & I - Q_3 \end{pmatrix} \cdot \begin{pmatrix} \Psi_S \circ T_S^A \\ \Psi_F \circ T_F^A \end{pmatrix} = \begin{pmatrix} Q_1 & Q_2 \\ 0 & Q_3 \end{pmatrix} \cdot \begin{pmatrix} \Psi_S \\ \Psi_F \end{pmatrix}. \quad (23)$$

We then obtain

$$\begin{cases} (I - Q_1) \cdot (\Psi_S \circ T_S^A) - Q_2 \cdot (\Psi_F \circ T_F^A) = Q_1 \cdot \Psi_S + Q_2 \cdot \Psi_F \\ 0 - (I - Q_3) \cdot (\Psi_F \circ T_F^A) = 0 + Q_3 \cdot \Psi_F \end{cases}. \quad (24)$$

Note that for the second equation in Eq. 24, we have had a solution from [4]. In particular, for  $j = 1, 2, \dots, 5$ , we have

$$\tau_{F_j}^A = -\tau_{F_1}^A \frac{\Psi_{F_1}}{\Psi_{F_j}} \sum_{k=1}^j \prod_{m=1}^k \gamma_m + \sum_{k=1}^j \sum_{l=1}^k \frac{\Psi_{F_l}}{\Psi_{F_j}} \frac{1}{P_{F_l, F_{l+1}}} \prod_{m=l+1}^k \gamma_m \quad (25)$$

We now look into the first equation in Eq. 24. Note that we have proved  $(I - Q_1)$  is reversible, then we have

$$T_S^A = (I - Q_1)^{-1} (Q_1 \cdot \Psi_S + Q_2 \cdot \Psi_F + Q_2 \cdot (\Psi_F \circ T_F^A)) \oslash \Psi_S, \quad (26)$$

where  $\oslash$  is the Hadamard division operator. And this equation is equivalent to

$$T_S^A = (I - Q_1)^{-1} [Q_1 \cdot (I - Q_1)^{-1} Q_2 \Psi_F + Q_2 \cdot \Psi_F + Q_2 \cdot (\Psi_F \circ T_F^A)] \oslash [(I - Q_1)^{-1} Q_2 \Psi_F]. \quad (27)$$

Due to the great complexity and verbose of the expression of  $F_2$ ,  $\tau_{S_1}^A$  and  $\tau_{S_2}^A$ , we do not present the analytic expressions here, but list the equation expansions around the neural selection, i.e.  $r = 1$ . It gives rise to

$$\begin{cases} \tau_{F_2}^A = \frac{832}{26} + \frac{312}{416}(r-1) - \frac{78650}{4992}(r-1)^2 + o((r-1)^3) \\ \tau_{S_1}^A = \frac{767}{26} + \frac{1125}{416}(r-1) - \frac{85409}{4992}(r-1)^2 + o((r-1)^3), \\ \tau_{S_2}^A = \frac{739}{26} + \frac{1422}{416}(r-1) - \frac{88001}{4992}(r-1)^2 + o((r-1)^3) \end{cases}, \quad (28)$$

Figure 5 shows the simulation results and the analytic curve. Note that the peaks of each curve are greater than the neural selection  $r = 1$ . We conclude several rules from the plot. i) At the neural selection  $r = 1$ , though the fixation probabilities for different mutant distances are the same, the times for mutant fixation are different. The greater distance two mutants have, the faster it takes for the mutant to fixate. An intuitive explanations is that as the distance between two mutants grows, each mutant becomes a more independent infection. And more infection sources lead to the faster mutant fixation. For instance, when two mutants are connected ( $d = 0$ ), there are only two wild-type individuals could be infected. On the contrary, when  $d = 2$ , there are totally four wild-type individuals are neighbors to the mutants. ii) When the mutants are at advantage ( $r > 1$ ), the time for mutant fixation and the fixation probability are nontrivial. On the one hand, for each mutant distance, the time to mutant fixation grows at first and decrease as the mutant fitness  $r$  grows. On the other hand, given a constant mutant fitness  $r$ , when distance between two mutants  $d$  becomes greater, the fixation time grows while the fixation probability changes non-monotonically (it decreases to the least when  $d = 1$  and grows when  $d > 1$ ). iii) When the mutants are disadvantageous ( $r < 1$ ), mutants fixate faster and with a better chance as the distance between two mutants grows. In general, the time for mutant fixation and the fixation probability do not hold a coordination relationship and the rank of times for mutant fixation is determined by the clustering factor (i.e., the distance between mutants).

## Separated Mutants For Large Circles

We now look into processes in larger circles. In general, we denote the population size as  $N$ . As Fig. 6 illustrated, we find that each state corresponds to a three-tuple  $(x, a, b)$ :  $x$  is the minimal distance of two mutant groups,  $a$  is the population size of the smaller mutant group and  $b$  is the population size of the larger mutant group. Note that the larger distance between two mutant groups equal to  $N - x - a - b$ .

All the states for general processes are listed in Table 1 for a population of size  $N$ . Similar as the previous section, we divide the states into the middle-state set  $S$  and the final-state set  $F$ . When the minimal distance  $x$  between two mutant groups is zero ( $x = 0$ ), or when the number of one of the mutant groups is 0 ( $a = 0$ ), we use  $F$  to replace the three-tuple expression  $S_{x,a,b}$  ( $S_{0,a,b} = F_{a+b}$  and  $S_{x,0,b} = F_b$ ). The middle states have two separate mutant groups whereas the final states only have one. From the table, we acknowledge that the total number of states is

$$\sum_{w=0}^N \left\lfloor \frac{w}{2} \right\rfloor \cdot \left\lfloor \frac{N-w}{2} \right\rfloor + N + 1. \quad (29)$$

This formula is strictly less than the one that removes the floor functions. Since  $(\sum_{w=0}^N \frac{w}{2} \cdot \frac{N-w}{2} + N + 1)$  is  $O(N^2)$ , it is acknowledged that the total number of states is of  $O(N^2)$ , which rises the difficulty of calculating the fixation probabilities with the equation  $\Psi P = \Psi$ .

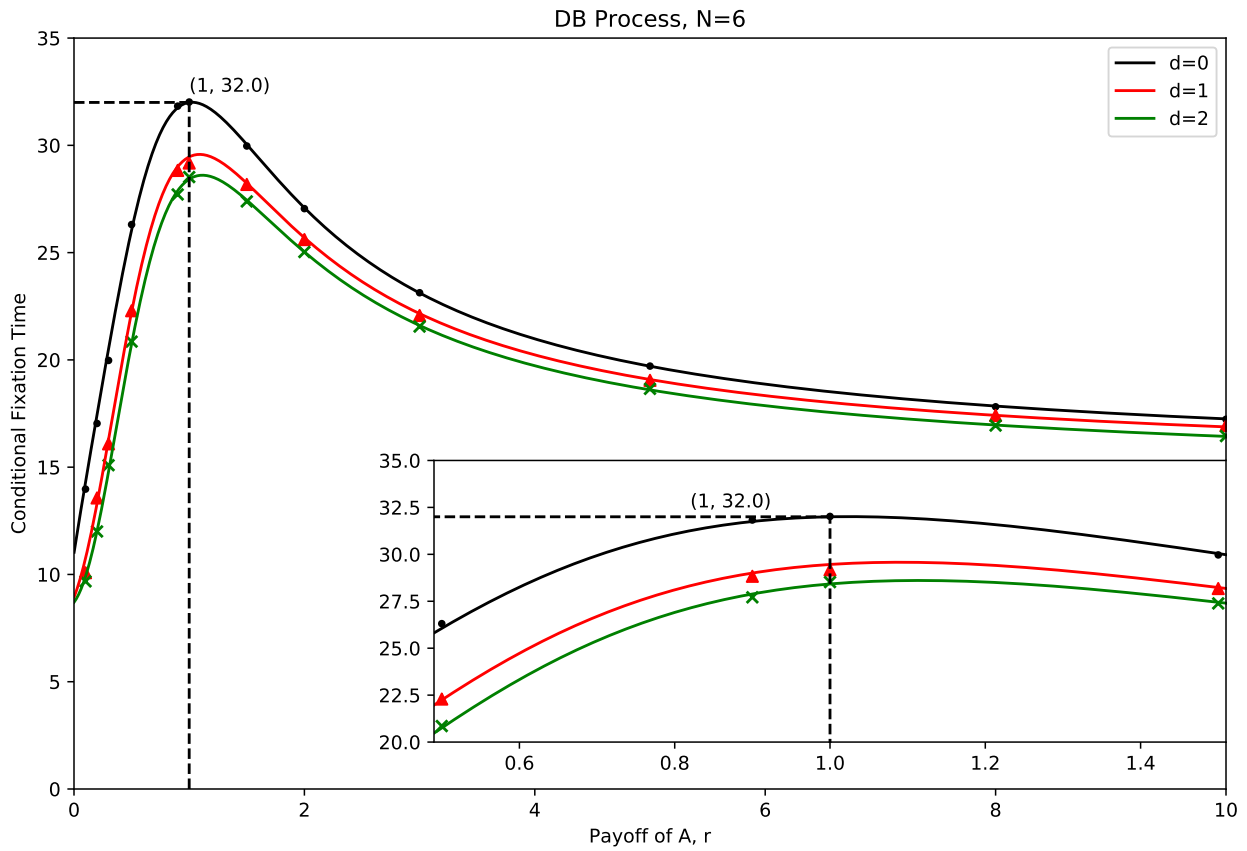


**Fig 5.** The time for mutant fixation in population size  $N = 6$ . The curve is the theoretical fixation time and the scatters are simulation results. The iteration time for simulation is 100,000.

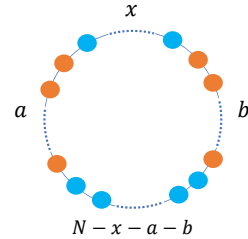


**Fig 6.**  $x, a, b$  refer to the minimal distance of two mutant groups, the population sizes of the smaller group and that of the larger one respectively. Each state can be denoted by the three-tuple uniquely. The following inequations holds:  $a \leq b$  and  $x \leq N - x - a - b$ .

For every transition between the states in Table 1, the state  $S_{x,a,b}$  stays where it is, or transits to a state where the mutant number is one greater or one less. Note that the number of mutant equals the sum of two mutant groups  $a + b$ . Take an example for  $S_{1,1,1}$ , it can transit itself,  $S_{1,1,2}$ ,  $S_{2,1,2}$  or  $F_1 (= S_{1,0,1})$ . We find that the number of transition is limited since the state transition only occurs when an individual at the

**Table 1.** The list of all the states in the process of population size  $N$ .  $w$  refers to the mutant number.

$w = 0$	1	2	3	4	$\dots$	$w$	$\dots$	$N$
$F_0$	$F_1$	$F_2$	$F_3$	$F_4$	$\dots$	$F_w$	$\dots$	$F_N$
		$S_{1,1,1}$	$S_{1,1,2}$	$S_{1,1,3}$	$S_{1,2,2}$	$\dots$	$S_{1,1,w-1}$	$\dots$
		$S_{2,1,1}$	$S_{2,1,2}$	$S_{2,1,3}$	$S_{2,2,2}$	$\dots$	$S_{2,1,w-1}$	$\dots$
		$\dots$	$\dots$	$\dots$	$\dots$	$\dots$	$\dots$	$\dots$
		$S_{\lfloor \frac{N-2}{2} \rfloor, 1, 1}$	$S_{\lfloor \frac{N-3}{2} \rfloor, 1, 2}$	$S_{\lfloor \frac{N-4}{2} \rfloor, 1, 3}$	$S_{\lfloor \frac{N-4}{2} \rfloor, 2, 2}$	$\dots$	$S_{\lfloor \frac{N-w}{2} \rfloor, 1, w-1}$	$\dots$
							$S_{\lfloor \frac{N-w}{2} \rfloor, \lfloor \frac{w}{2} \rfloor, w-\lfloor \frac{w}{2} \rfloor}$	

border of a group is chosen to die. As the mutants and wild-type individuals have one or two groups respectively, there are at most 8 individuals on the border. That is to say, starting from any state, there are at most 8 transitions. When the population size  $N$  is large, the transition matrix must be sparse. We list all the transition probabilities and boundary conditions in Table 2.

**Table 2.** Non-zero one-step transition probabilities for  $S_{x,a,b}$ . Note that destination states in the left column might not hold inequations  $a \leq b$  and  $x \leq N - x - a - b$ . When the inequations is broken, we need to exchange  $a$  and  $b$  or exchange  $x$  and  $N - x - a - b$ .

$P$	$N - x - a - b = 1$	$x = 1$	$a = 1$	$b = 1$	<i>otherwise</i>
$F_{a+b+1}, \#1$	$\frac{1}{N}$	$\frac{1}{N}$	0	0	0
$F_a, \#2$	0	0	$\frac{1}{N}$	0	0
$F_b, \#3$	0	0	0	$\frac{1}{N}$	0
$S_{x,a+1,b}, \#4$	0	$\frac{1-r}{N-1+r}$	$\frac{1-r}{N-1+r}$	$\frac{1-r}{N-1+r}$	$\frac{1-r}{N-1+r}$
$S_{x,a,b+1}, \#5$	0	$\frac{1-r}{N-1+r}$	$\frac{1-r}{N-1+r}$	$\frac{1-r}{N-1+r}$	$\frac{1-r}{N-1+r}$
$S_{x-1,a+1,b}, \#6$	$\frac{1-r}{N-1+r}$	0	$\frac{1-r}{N-1+r}$	$\frac{1-r}{N-1+r}$	$\frac{1-r}{N-1+r}$
$S_{x-1,a,b+1}, \#7$	$\frac{1-r}{N-1+r}$	0	$\frac{1-r}{N-1+r}$	$\frac{1-r}{N-1+r}$	$\frac{1-r}{N-1+r}$
$S_{x,a-1,b}, \#8$	$\frac{1}{N-1+r}$	$\frac{1}{N-1+r}$	0	$\frac{1}{N-1+r}$	$\frac{1}{N-1+r}$
$S_{x+1,a-1,b}, \#9$	$\frac{1}{N-1+r}$	$\frac{1}{N-1+r}$	0	$\frac{1}{N-1+r}$	$\frac{1}{N-1+r}$
$S_{x,a,b-1}, \#10$	$\frac{1}{N-1+r}$	$\frac{1}{N-1+r}$	$\frac{1}{N-1+r}$	0	$\frac{1}{N-1+r}$
$S_{x+1,a,b-1}, \#11$	$\frac{1}{N-1+r}$	$\frac{1}{N-1+r}$	$\frac{1}{N-1+r}$	0	$\frac{1}{N-1+r}$
$S_{x,a,b}$	$1 - \sum \text{column}$				

We find that the general process shares four properties with the process of a population size 6 in the last section. i) The middle states can reach any other middle states and they belong to one equivalent class. Take the transition from  $S_{1,1,1}$  to  $S_{2,2,2}$  for an instance, there is a path as  $S_{1,1,1} \rightarrow S_{1,1,2} \rightarrow S_{2,1,1} \rightarrow S_{2,1,2} \rightarrow S_{2,2,2}$ . In this path, the transition number in Table 2 occurs in an order as  $\#5 \rightarrow \#11 \rightarrow \#5 \rightarrow \#4$ . ii) The final states can also reach any other final states and the final-state-set contains another equivalent class ( $F_w, 1 \leq w \leq N - 1$ ) and two absorbing states ( $F_0$  and  $F_N$ ). iii) The middle states can reach final states in limited time, however the final states cannot reach any of the middle states. iv) As the middle states might transit to the final states and cannot return itself, the middle states are transient.

With four properties from i) to iv), it shows the derivations from Eq. (11) to Eq. (16) hold. We can obtain the fixation probabilities for the general process by

$$\Psi_S = (I - Q_1)^{-1} Q_2 \Psi_F, \quad (30)$$

where  $Q_1$  and  $\Psi_F$  is dependent on the relative mutant fitness  $r$  and  $Q_2$  is independent from  $r$ . And similarly, we are able to obtain the time for mutant fixation for large populations as

$$T_S^A = (I - Q_1)^{-1} [Q_1 \cdot (I - Q_1)^{-1} Q_2 \Psi_F + Q_2 \cdot \Psi_F + Q_2 \cdot (\Psi_F \circ T_F^A)] \otimes [(I - Q_1)^{-1} Q_2 \Psi_F]. \quad (31)$$

In S2 Appendix, we develop an algorithm to obtain the numerical  $Q_1$  and  $Q_2$  with a time complexity of  $O(N^2)$  and a time complexity of  $O(N^4)$  ( $O(N^2)$  if sparse matrix method is employed). Combining with Eq. (30) and Eq. (31), we obtain the fixation probabilities and fixation times for any population size  $N$ . As there are several matrix multiplications and matrix inversions in the algorithm, the final time complexity for obtaining fixation probability and fixation time are the same as  $O(N^{4.746})$  [5, 6].

In particular, with Taylor's expansion around  $r = 1$  for Eq. (30), we have

$$\Psi(r) = \Psi(1) + \frac{d}{dr}\Psi(r)\bigg|_{r=1}(r-1) + \frac{1}{2}\frac{d^2}{dr^2}\Psi(r)\bigg|_{r=1}(r-1)^2 + o((r-1)^2), \quad (32)$$

where

$$\frac{d}{dr}\Psi(r) = [I - Q_1(r)]^{-1}\frac{d}{dr}Q_1(r)[I - Q_1(r)]^{-1}Q_2\pi(r) + [I - Q_1(r)]^{-1}Q_2\frac{d}{dr}\pi(r), \quad (33)$$

$$\begin{aligned} \frac{d^2}{dr^2}\Psi(r) &= 2[I - Q_1(r)]^{-1}\frac{d}{dr}Q_1[I - Q_1(r)]^{-1}\frac{d}{dr}Q_1(r)[I - Q_1(r)]^{-1}Q_2\pi(r) \\ &\quad + [I - Q_1(r)]^{-1}\frac{d^2}{dr^2}Q_1(r)[I - Q_1(r)]^{-1}Q_2\pi(r) \\ &\quad + 2[I - Q_1(r)]^{-1}\frac{d}{dr}Q_1(r)[I - Q_1(r)]^{-1}Q_2\frac{d}{dr}\pi(r) \\ &\quad + [I - Q_1(r)]^{-1}Q_2\frac{d^2}{dr^2}\pi(r). \end{aligned} \quad (34)$$

The detail of the expansion is in S3 Appendix. And the algorithm we developed also applies to calculate the derivatives of the fixation probabilities. We explain it in detail in S4 Appendix.

The fixation probabilities for different mutant distances  $d$  are illustrated in Fig. 7, where the population size is 25. Some values of mutant group distance ( $d = 4, 5, \dots, 10$ ) are ignored for clarification of the figure. We list the accurate numeric fixation probabilities and their derivatives in Table 3 for population size  $N = 6, 25, 100$  respectively. For all the population sizes we have explored, the features follow that in Fig. 4: i) The fixation probabilities equal to the population size fraction at the neural selection, i.e.,  $r = 1$ . ii) The first-order derivatives for separated mutants ( $d > 1$ ) are the same. iii) The first-order derivatives for the connected mutants are greater than that of the separated mutants. Thus, connected mutants weaken the invasion when mutants are at advantage and promote the invasion when they are at disadvantage. In particular, for population sizes we have explored ( $N = 6, 25$  and  $100$ , and more results on different population sizes can be found at [7]), the first-order derivatives of fixation probabilities at the neural selection  $r = 1$  obey the following:

$$\begin{cases} \frac{d}{dr}\Psi_{F_2}(=\Psi_{S_{0,1,1}})\bigg|_{r=1} = \frac{2N-5}{2N} \\ \frac{d}{dr}\Psi_{S_{d,1,1}}\bigg|_{r=1} = \frac{2N-6}{2N} \quad , d = 1, 2, \dots, \lfloor \frac{N-2}{2} \rfloor \end{cases}. \quad (35)$$

We believe that this applies to  $\forall N \geq 6$ , but the proof is still an open issue. iv) The second-order fixation probabilities for the separated mutants increase as the distance  $d$  grows. Thus, as the mutants are not initially connected, the rank of the invasion chance is determined only by the clustering factor (i.e., the distance between two mutants at the beginning). The greater distance two mutants are, the greater fixation probabilities they have. Note that for the process from  $N = 6$  to  $N = 25$ , the second order derivatives become greater than zero and the curves turn from convex to concave.

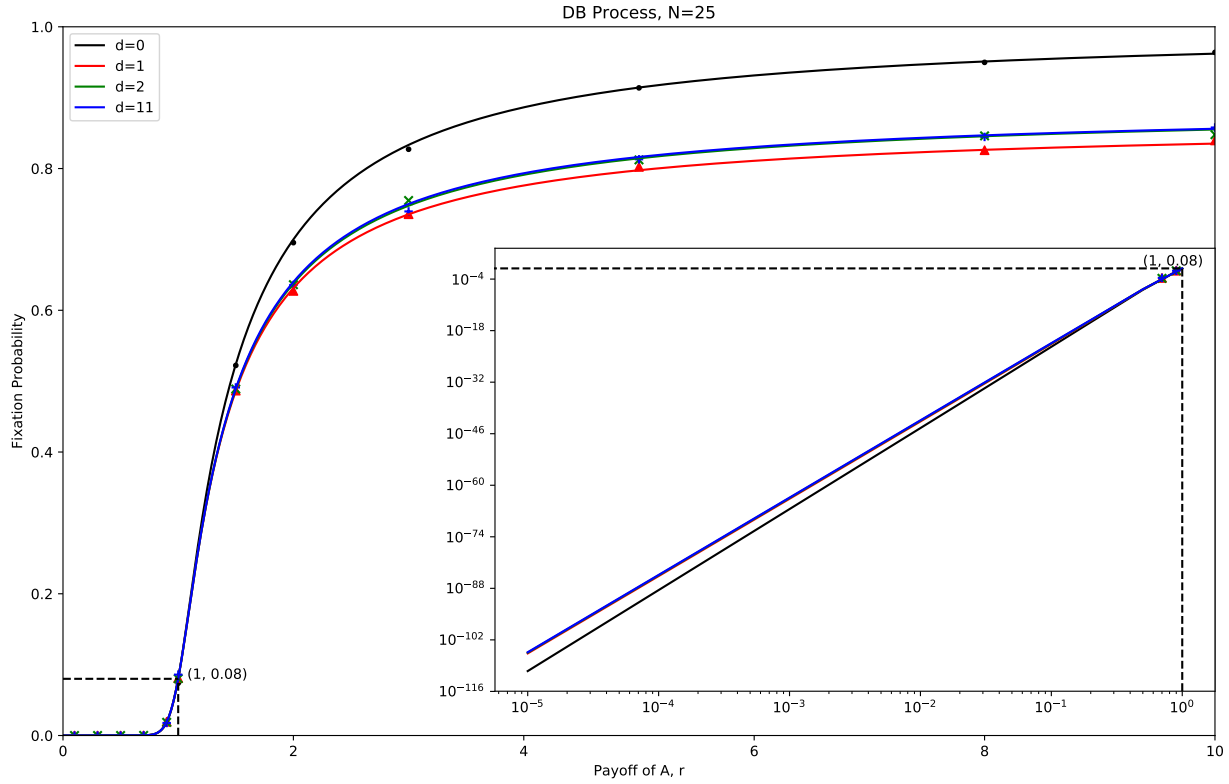


**Fig 7.** The fixation probability for  $N = 25$  with different initial mutant distances  $d$ . The curve is drawn by the results calculated by our developed algorithm whereas the points are simulation results. Note that the fixation probability for  $r \leq 0.5$  is too small and they are 0 in the simulation results. Hence they are not drawn in the subfigure.

**Table 3.** The transition probabilities and their derivatives for  $S_{d,1,1}$ , whereas  $0 \leq d \leq \lfloor \frac{N-2}{2} \rfloor$ .  $N$  refers to the population size.

$N$	6			25			100			
	$d$	$\Psi_{S_{d,1,1}}$	$\frac{d}{dr}\Psi_{S_{d,1,1}}$	$\frac{d^2}{dr^2}\Psi_{S_{d,1,1}}$	$\Psi_{S_{d,1,1}}$	$\frac{d}{dr}\Psi_{S_{d,1,1}}$	$\frac{d^2}{dr^2}\Psi_{S_{d,1,1}}$	$\Psi_{S_{d,1,1}}$	$\frac{d}{dr}\Psi_{S_{d,1,1}}$	$\frac{d^2}{dr^2}\Psi_{S_{d,1,1}}$
0	0	0.333	0.583	-0.138	0.08	0.9	2.5648	0.02	0.975	29.9098
1	1	0.333	0.5	-0.170	0.08	0.88	2.37115	0.02	0.97	14.71808826
2	2	0.333	0.5	-0.160	0.08	0.88	2.37492	0.02	0.97	14.71902959
3	3	-	-	-	0.08	0.88	2.37639	0.02	0.97	14.7193983
...	...	...	...	...	...	...	...	...	...	...
10	10	-	-	-	0.08	0.88	2.37807	0.02	0.97	14.71983193
11	11	-	-	-	0.08	0.88	2.37809	0.02	0.97	14.71984276
12	12	-	-	-	-	-	-	0.02	0.97	14.7198512
...	...	...	...	...	...	...	...	...	...	...
48	48	-	-	-	-	-	-	0.02	0.97	14.71989511
49	49	-	-	-	-	-	-	0.02	0.97	14.71989512

And Figure 8 shows the simulation results of the time for mutant fixation and the numerical curve for population size  $N = 25$ . Similarly to the results of the small circle, we find three major rules: i) The times for mutant fixation are different while the

fixation probabilities are not at the neural selection. The rank of the conditional fixation time is determined by the distance between two initial mutants. ii) When the mutants are at advantage ( $r > 1$ ), the time for mutant fixation grows at first and decrease as the mutant fitness  $r$  grows. And given a constant mutant fitness  $r$ , the fixation time does not coordinate with the fixation probability. The greater distance between mutants  $d$  is, the faster the mutants fixate, but the chance of fixation bumps. iii) When the mutants are at disadvantage ( $r < 1$ ), the mutants fixate faster and with a better chance as the distance between two mutants grows.

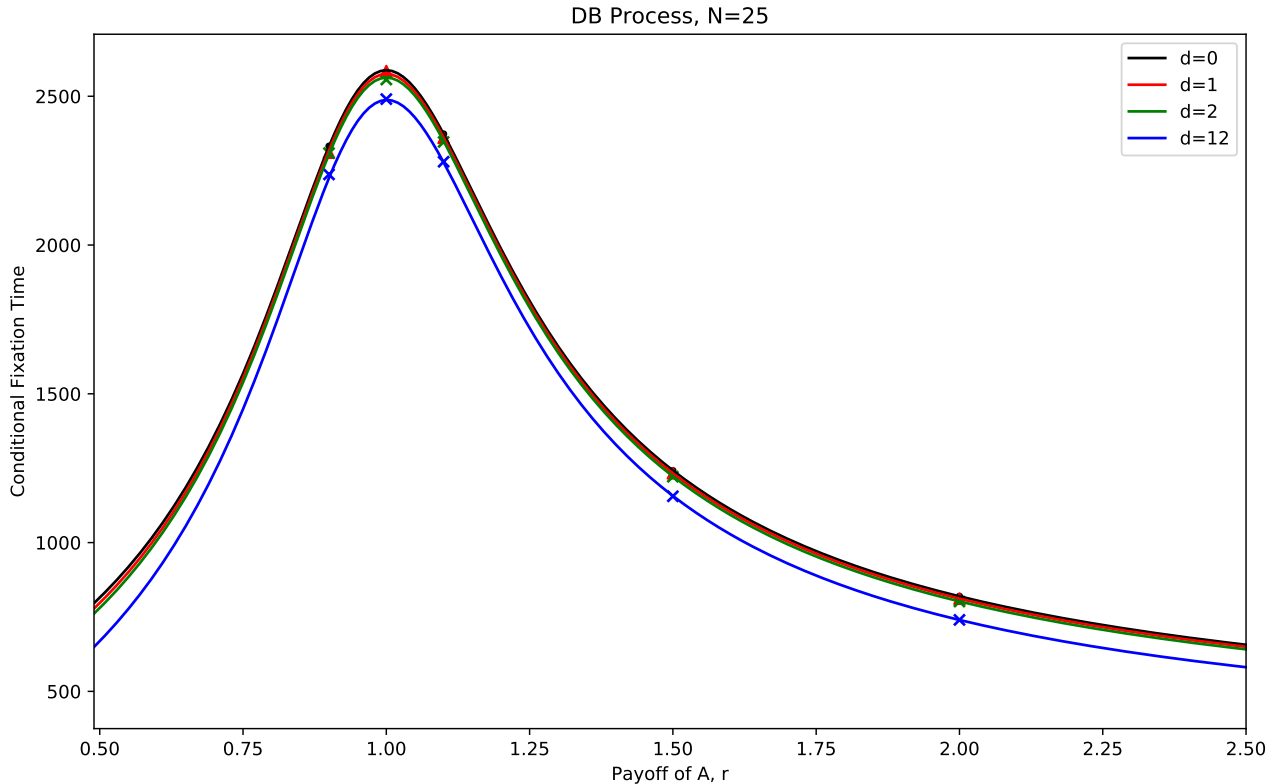


**Fig 8.** The time for mutant fixation in population size  $N = 25$  with different initial mutant distances  $d$ . The curve is drawn by the numerical results from our developed algorithm and scatters are simulation results. The iteration time for simulation is 1,000,000.

## Discussion

A mechanism developed by many is the assortment interactions [14, 15]. It does not assume that individuals always play randomly but strategically. They try to choose associates that maximize the group payoff. David et al. [14] show that the assortment interactions lead to clustering of the similar individuals, and finally lead to increasing variation among groups, which affects the balance of selections. This behavior fits the intuitive for the clustering of similar individuals. The tag-based dynamics is a related topic, where individuals try to choose the associates who are similar to themselves, or say they try to choose associates that maximize self-interests. They denote to the others who are in their tolerance. Tag-based donation can lead to the emergence of

cooperation [8], where clustering occurs during the process. Specifically, the clustering of individuals with similar tags lead to high donation rates and thus enhance the cluster payoff. Again, the clustering here shows itself as an important intermediate process.

We implemented a minimal model as adopting a simple circle as the spatial structure and applied the frequency-independent cases. And we set the fitness of each individual to be only related to the strategy it chooses. There would be no game for each update, and we put more focus on the distance between mutants. Thus we disentangle the clustering and the games.

We evaluate the process for a population of size 6. The analytical and simulation results show that initially fully connected individuals adopting one strategy would enhance the group survival when they are at advantage while weakening it when at disadvantage. This result fits the intuitive. The assortment is an amplifier of the selection for the connected mutants compared with separated mutants. However, as long as two mutants are separated, the relative mutant fitness  $r$  does not determine the rank of the probability of successful invasion, but the clustering factor (the distance between two mutants) does. Denoting  $d$  as the initial distance between two mutant individuals, the fixation probability falls to the least when  $d = 1$ , and it grows as  $d$  becomes greater. That is to say, the greater distance the initial two mutants have, the greater the invasion chance is, no matter mutants are at advantage or not. Our results show that the effect of clustering appears as very fundamental and far-reaching in the DB process.

We analyzed the fixation probabilities and their derivatives in a two-stage method and developed an algorithm for the calculation of separated mutants for the general cases. The algorithm has a time complexity of  $O(N^{4.746})$  and a space complexity of  $O(N^4)$ , or  $O(N^2)$  if sparse matrix methods are adopted. We evaluated the processes for greater population sizes of 25 and 100. The features in the small circle still apply. Without loss of a generality, we consider the features apply to any population size, where strict proof of the features is still an open issue. And there might be some similarities for processes in more complex spatial structures.

Some previous studies [9] have looked into the invasion for different games in a lattice. Feng et al. compared with the snowdrift game and the prisoner's dilemma. In the simulation, two games perform different pattern on the invasion under the same other conditions. As the ratio of cost and benefit grows, The mutants tend to emerge as several compact clusters in the prisoner's dilemma whereas the mutants evolve to many discrete clusters. The games are involved in the study whereas the clustering is not. We explored the opposite question.

Our results are different from that in the spatial dynamics of Martin A. Nowak [10], where they proved that the clustering does not play a role in determining the chance of mutant invasion in BD process. The difference might enlighten some more details for the difference between the DB and BD process. And it shows that the clustering effect might be highly related to the process of updating.

And in the work of Ohtsuki et al. [2], they use pair approximations by considering the fixation possibilities are the same for the graphs with the same pair relations. Or say that they adopted the statistical average for all the cases with the same pair relations. The pair relation refers to that the chance of finding a mutant next to a mutant  $q_{A|A}$  or finding a wild-type individual next to a mutant  $q_{B|A}$ . For example, let's assume that there are 25 individuals on a ring and two of them are mutants. When the distance between two mutants are equal or greater than two ( $2 \leq d \leq 12$ ), all the cases share the same probability of finding a mutant next to a wild-type individual ( $q_{B|A} = \frac{4}{23}$ ) or finding a wild-type individual next to a wild-type individual ( $q_{A|A} = 1$ ). However, in our simulation and analytical results, the fixation probabilities are not the same for different mutant distances. We further find that the difference occurs at the second-order derivative level. This suggests that the pair relation cannot be the sole

factor to portray the clustering accurately.

In general, our results reveal quite unintuitive but fundamental effect of clustering in the DB process. The clustering plays its role without the involvement of games. It is not hard to imagine the great complexity when different games are involved and more complex graphs are introduced, and it deserves some further studies to the extensions to better understand the pattern and solely effect of clustering.

## Supporting information

**S1 File. Python program.** We implemented our developed algorithm in a Python program to calculate the theoretical fixation probabilities and the derivatives. The code is available at [https://github.com/Awdrtgg/DB\\_on\\_cycle/blob/master/fp\\_and\\_derivatives.py](https://github.com/Awdrtgg/DB_on_cycle/blob/master/fp_and_derivatives.py).

**S2 File. Python program.** We implemented our developed algorithm in a Python program to calculate the theoretical conditional fixation times. The code is available at [https://github.com/Awdrtgg/DB\\_on\\_cycle/blob/master/fixation\\_time.py](https://github.com/Awdrtgg/DB_on_cycle/blob/master/fixation_time.py).

**S3 File. Python program.** We evaluated the fixation probabilities and fixation times by simulating the process in a Python program. The simulation code is available at [https://github.com/Awdrtgg/DB\\_on\\_cycle/blob/master/simulation.py](https://github.com/Awdrtgg/DB_on_cycle/blob/master/simulation.py).

**S1 Appendix. Algorithm for transformation between the state number and the three-tuple.** Functions *tuple\_to\_state* and *state\_to\_tuple* shows the correspondences between the three-tuple and the state number in the middle states.

---

**Algorithm 1** *tuple\_to\_state*( $n, x, a, b$ ) for mapping tuple to state

---

**Input:**

The total individual number  $n$ ;  
The triad  $x, a, b$ ;

**Output:** *state*

```
1: if  $a > b$  then
2:   swap( $a, b$ ) // Constrain
3: end if
4: if  $x > n - a - b$  then
5:    $x \leftarrow n - a - b$  // Constrain
6: end if
7: if  $x = 0$  then
8:   return  $F_{a+b}$ 
9: end if
10: if  $a = 0$  then
11:   return  $F_b$ 
12: end if
13:  $i \leftarrow 0$ 
14: for  $w \leftarrow 0$  to  $(a + b)$  do
15:    $i \leftarrow i + \lfloor \frac{w}{2} \rfloor \cdot \lfloor \frac{n-w}{2} \rfloor$ 
16: end for
17:  $i \leftarrow i + (a - 1) \cdot \lfloor \frac{n-a-b}{2} \rfloor$ 
18:  $i \leftarrow i + x - 1$ 
19: return  $S_i$ 
```

---

---

**Algorithm 2** state\_to\_tuple( $i$ ) for mapping state number to tuple

---

**Input:**The number  $i$ ;**Output:**  $x, a, b$ 

```
1:  $a \leftarrow 1$ 
2:  $w \leftarrow 0$ 
3: while  $i \geq \lfloor \frac{w}{2} \rfloor \cdot \lfloor \frac{n-w}{2} \rfloor$  do
4:    $i \leftarrow i - \lfloor \frac{w}{2} \rfloor \cdot \lfloor \frac{n-w}{2} \rfloor$ 
5:    $w \leftarrow w + 1$  // To get the weight
6: end while
7: while  $i \geq \lfloor \frac{n-w}{2} \rfloor$  do
8:    $i \leftarrow i - \lfloor \frac{n-w}{2} \rfloor$ 
9:    $a \leftarrow a + 1$  // To get the column
10: end while
11:  $b \leftarrow w - a$ 
12:  $x \leftarrow i + 1$ 
13: return  $x, a, b$ 
```

---

**S2 Appendix. The algorithm to calculate the fixation probabilities.** After iterating all the transitions for each state, we obtain the transition matrix  $P$ . As each state requires a computation with time complexity of  $O(1)$  (8 possible cases as Table 2 shows), it costs a time of complexity  $O(N^2)$  to iterate all the states. Algorithm 3 gives the process of calculation for  $Q_1$  and  $Q_2$ . The time complexity and space complexity of the algorithm are  $O(N^2)$  and  $O(N^4)$  respectively. Note that  $Q_1$  and  $Q_2$  are sparse matrices when  $N$  is great. Therefore, the space complexity is  $O(N^2)$  if sparse storing methods are adopted.

---

**Algorithm 3** Calculation of  $Q_1$  and  $Q_2$ 


---

**Input:**

Total individual number  $N$ ;  
 Mutant payoff  $r$ ;

**Output:**  $Q_1, Q_2$ 

```

1: Total  $\leftarrow 0$ 
2: for  $w \leftarrow 0$  to  $N + 1$  do
3:   Total  $\leftarrow$  Total +  $\lfloor \frac{w}{2} \rfloor \cdot \lfloor \frac{n-w}{2} \rfloor$ 
4: end for
5:  $Q_1 \leftarrow [0]_{Total \times Total}$ 
6:  $Q_2 \leftarrow [0]_{Total \times (N+1)}$ 
7: for  $i \leftarrow 1$  to Total do
8:   prob_self  $\leftarrow 1$  // The possibility of staying where it is
9:   for  $j \leftarrow 1$  to 11 do
10:     $x, a, b \leftarrow state\_to\_tuple(i)$ 
11:    Change  $x, a, b$  by corresponding  $\#j$ 
12:     $t \leftarrow tuple\_to\_state(n, x, a, b)$ 
13:    temp_prob  $\leftarrow prob \#j$ 
14:    if  $t \in F$  then
15:       $Q_2[S_i, t] \leftarrow Q_2[S_i, t] + temp\_prob$ 
16:    else
17:       $Q_1[S_i, t] \leftarrow Q_1[S_i, t] + temp\_prob$ 
18:    end if
19:    prob_self  $\leftarrow prob\_self - temp\_prob$ 
20:  end for
21:   $Q_1[S_i, S_i] \leftarrow Q_1[S_i, S_i] + prob\_self$ 
22: end for
23: return  $Q_1, Q_2$ 

```

---

**S3 Appendix. The first and second order derivative of fixation probability.**

In the following, we give the details of calculating the first-order derivatives and the second-order derivatives of the fixation probability  $\Psi$ . In general, we have

$$\Psi(r) = [I - Q_1(r)]^{-1} Q_2 \pi(r). \quad (36)$$

Where  $I$  is an identity matrix of the same size with  $Q_1$ . The derivation of  $\Psi$  is

$$\frac{d}{dr} \Psi(r) = \frac{d}{dr} [I - Q_1(r)]^{-1} Q_2 \pi(r) + [I - Q_1(r)]^{-1} Q_2 \frac{d}{dr} \pi(r). \quad (37)$$

Since we have the analytical result for  $\pi(r)$ , the second part of the right side of equation is acknowledged. The point of the problem comes to  $\frac{d}{dr} [I - Q_1(r)]^{-1}$ .

The property of the matrix inversion gives rise to

$$[I - Q_1(r)]^{-1} [I - Q_1(r)] = I. \quad (38)$$

The derivations of both sides of the equation is

$$\frac{d}{dr} [I - Q_1(r)]^{-1} [I - Q_1(r)] + [I - Q_1(r)]^{-1} \frac{d}{dr} [I - Q_1(r)] = 0. \quad (39)$$

This is equivalence to

$$\frac{d}{dr} [I - Q_1(r)]^{-1} [I - Q_1(r)] = [I - Q_1(r)]^{-1} \frac{d}{dr} Q_1(r). \quad (40)$$

Multiply  $[I - Q_1(r)]^{-1}$  for both sides, we have

$$\frac{d}{dr}[I - Q_1(r)]^{-1} = [I - Q_1(r)]^{-1} \frac{d}{dr}Q_1(r)[I - Q_1(r)]^{-1}. \quad (41)$$

Taking Eq. (41) into Eq. (37) results in

$$\frac{d}{dr}\Psi(r) = [I - Q_1(r)]^{-1} \frac{d}{dr}Q_1(r)[I - Q_1(r)]^{-1}Q_2\pi(r) + [I - Q_1(r)]^{-1}Q_2 \frac{d}{dr}\pi(r), \quad (42)$$

And the second-order derivative Eq. (34) can be obtained similarly.

**S4 Appendix. Apply the algorithm to calculate the derivatives of fixation probabilities.** The derivative of a matrix is defined as the matrix of derivatives of corresponding item. With acquiring  $\frac{d}{dr}Q_1(r)$  by turning values in Table 2 into their first order derivatives and running through Algorithm 3, the first-order derivatives of the fixation probabilities are obtained combining with Eq. (33). Besides, the time complexity is not changed since calculation of  $\frac{d}{dr}Q_1(r)$  follows that of  $Q_1$  and they have the same complexity. Several matrices multiplications and additions are needed but they would not increase the time complexity to a higher order. The required space would double but it is still of a complexity  $O(N^4)$  ( $O(N^2)$  for adopting sparse matrices). Similarly, we find that the higher order derivatives of the fixation probabilities include the variables required by the lower derivative and the derivative of  $Q_1$  of its order. We could thus obtain the second order derivatives and higher order ones by turning the values in Table 12 to their higher order derivatives. The overall complexity will stay the same.

## Acknowledgments

This work is supported by NSFC (Grants No. 61603049, No. 61751301) and the Fundamental Research Funding for the Central Universities in China (No. 2017RC19).

## References

1. Nowak MA. Five rules for the evolution of cooperation. *science*. 2006 Dec 8;314(5805):1560-3.
2. Ohtsuki H, Hauert C, Lieberman E, Nowak MA. A simple rule for the evolution of cooperation on graphs and social networks. *Nature*. 2006 May;441(7092):502.
3. Grimmett G and Stirzaker D. (2009). *Probability and random processes*. Oxford: Oxford Univ. Press, pp.221-224.
4. Traulsen A, Hauert C. Stochastic evolutionary game dynamics. *Reviews of nonlinear dynamics and complexity*, 2, 25-61.
5. François Le Gall. Powers of tensors and fast matrix multiplication. *International Symposium on Symbolic and Algebraic Computation*. 2014 Jul 23 (pp. 296-303). ACM.
6. Coppersmith D, Winograd S. Matrix multiplication via arithmetic progressions. In *Proceedings of the nineteenth annual ACM symposium on Theory of computing*. 1987 January. (pp. 1-6). ACM.

7. The repository for theoretical fixation probabilities and derivatives for different population size, [https://github.com/Awdrtgg/DB\\_on\\_cycle/tree/master/algorithm-result](https://github.com/Awdrtgg/DB_on_cycle/tree/master/algorithm-result).
8. Riolo R L, Cohen M D, Axelrod R. (2001). Evolution of cooperation without reciprocity. *Nature*, 414(6862), 441.
9. Fu F, Nowak M A, Hauert C. Invasion and expansion of cooperators in lattice populations: Prisoner's dilemma vs. snowdrift games. *Journal of theoretical biology*, 266(3), 358-366.
10. Lieberman E, Hauert C, Nowak MA. Evolutionary dynamics on graphs. *Nature*. 2005 Jan;433(7023):312.
11. Ohtsuki H, Nowak MA. Evolutionary games on circles. *Proceedings of the Royal Society of London B: Biological Sciences*. 2006 Sep 7;273(1598):2249-56.
12. Kaveh K, Komarova NL, Kohandel M. The duality of spatial death–birth and birth–death processes and limitations of the isothermal theorem. *Royal Society open science*. 2015 Apr 1;2(4):140465.
13. Hamilton WD. The genetical evolution of social behaviour. I. *Journal of Theoretical Biology*. 1964 Jul; 7(1):1-16.
14. Toro M Silio, L. Assortment of encounters in the two-strategy game. *Journal of theoretical biology*, 1986; 123(2), 193-204.
15. Wilson D S, Dugatkin L A. Group selection and assortative interactions. *The American Naturalist*. 1997; 149(2), 336-351.